

Non-parametric Mitigation of Periodic Impulsive Noise in Narrowband Powerline Communications

Jing Lin and Brian L. Evans

Wireless Networking and Communications Group
The University of Texas at Austin, Austin, TX 78712 USA
Email: jing.lin@utexas.edu, bevans@ece.utexas.edu

Abstract—Periodic impulsive noise synchronous to the main powerline frequency is the dominant noise component in OFDM-based narrowband (NB) powerline communications (PLC). Such noise occurs in periodic bursts, where a single burst could corrupt multiple OFDM symbols. Standardized NB PLC systems use frequency-domain interleaving (FDI) in combination with forward error correction to combat impulsive noise. Alternate designs adopt time-domain block interleaving (TDI) in which the receiver deinterleaver scatters an impulsive noise burst into short impulses over a large number OFDM symbols. In bursty impulsive noise, TDI-OFDM (FDI-OFDM) works better at high (low) SNR. In this paper, we develop non-parametric methods for periodic impulsive noise mitigation in coded TDI-OFDM systems. We exploit the sparse structure of the time-domain noise after the deinterleaver, and propose sparse Bayesian learning based algorithms that estimate and remove the noise impulses by observing the null and pilot tones of received signal and using decision feedback from the decoder. The proposed methods do not assume any statistical noise model and hence do not require any training. In simulations, the proposed methods in TDI-OFDM systems achieve up to 6 dB SNR gain over FDI-OFDM systems at typical NB PLC SNR values.¹

I. INTRODUCTION

Due to the high penetration of powerline infrastructures and hence low deployment costs, powerline communications (PLC) plays a prominent role in enabling a variety of smart grid applications, such as automatic meter reading, grid status control and monitoring, and real-time pricing [1]. In 2011, PLC was the most adopted (60% market share) technology in smart meters for communication with local utilities [2]. In particular, narrowband (NB) PLC is used for the communications between smart meters and data concentrators, which are deployed by local utilities on medium-voltage (in the US) or low-voltage (in Europe) power lines. NB PLC uses orthogonal frequency division multiplexing (OFDM) to deliver several hundred kbps in the 3–500 kHz band. Examples of NB PLC systems have been specified in the industry-developed standards such as G3 and PRIME, and recent international standards such as IEEE P1901.2 and ITU-T G.hnem.

One of the major challenges for NB PLC is to overcome additive powerline noise. Such noise is generated by electrical devices connected to the power lines, and by external noise and interference coupled to the power grids via radiation or conduction [1]. Recent field measurements on both indoor and

¹This work was supported by gift funding and equipment donations from National Instruments, as well as grant funding from the Semiconductor Research Corporation under SRC GRC Task 1836.063 with liaisons Freescale Semiconductor, IBM and Texas Instruments.

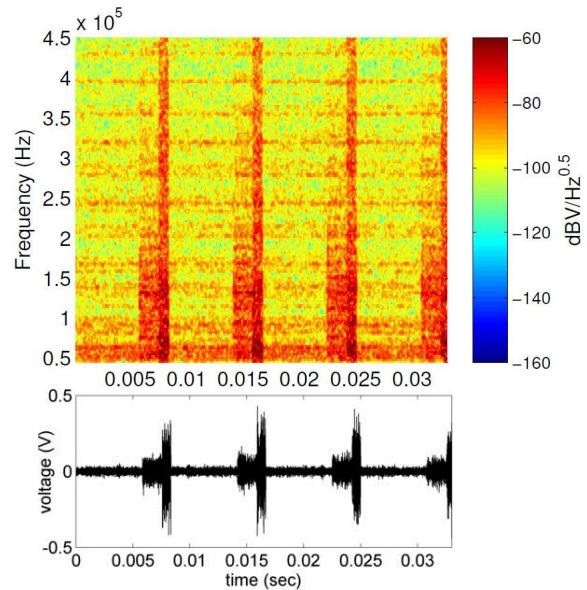


Fig. 1. Periodic impulsive noise synthesized from a linear periodically time varying system model adopted by the IEEE P1901.2 narrowband powerline communications standard. The noise exhibits cyclostationarity in both time domain (bottom) and frequency domain (top).

outdoor power lines have identified periodic impulsive noise (also termed “cyclostationary noise”) synchronous to the main powerline frequency as the dominant noise component in the 3–500 kHz band [3], [4], [5]. This type of noise contains long noise bursts that occur periodically with half the AC cycle. Typical noise bursts cover 10% – 30% of a period, which amounts to $833 \mu\text{s}$ – 2.5 ms in the US. A single noise burst may corrupt multiple consecutive OFDM symbols. For example, the OFDM symbol duration in G3 operating in the CENELEC-A band from 3–95 kHz [6] is $695 \mu\text{s}$, and a noise burst lasting for 30% of a period will contaminate up to 4 consecutive OFDM symbols. During the bursts, the noise power in certain frequency bands can reach 30–50 dB higher than in the rest of the period [4]. A primary source of periodic impulsive noise is switching mode power supplies (e.g. light dimmers and DC-DC converters) [5].

The temporal and spectral properties of periodic impulsive noise in NB PLC have been captured by a linear periodically time varying (LPTV) system model [4], which has been adopted by the IEEE P1901.2 NB PLC standard. According to the model, a period of the noise can be partitioned into several intervals, within each the noise is a stationary Gaussian process that is spectrally shaped by a linear time-invariant

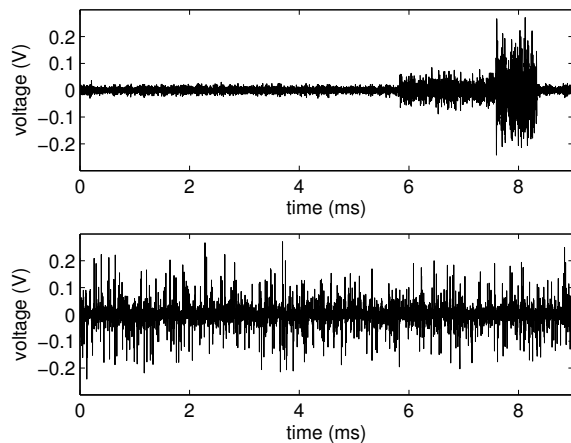


Fig. 2. Periodic impulsive noise before (top) and after (bottom) a time-domain block deinterleaver over one period of the noise.

filter. Fig. 1 shows a noise trace, along with its spectrogram, synthesized from an LPTV system model that is fitted to noise measurements collected at an outdoor low-voltage site [4].

Periodic impulsive noise may cause severe deterioration in communication performance at OFDM-based NB PLC receivers. Commercial PLC modems feature low power transmission [7], which is further attenuated by significant path loss over powerline channels [1]. The communication signal, if received during the impulsive noise bursts, could be overwhelmed and severely corrupted. Since statistics of the noise significantly deviates from that of additive white Gaussian noise (AWGN), additional degradation in communication performance can be expected at conventional OFDM receivers designed under the assumption of AWGN. Furthermore, since the bursty duration is comparable or even longer than the OFDM symbol duration, the corruption generally affects multiple consecutive OFDM symbols [8].

Standardized NB PLC systems use frequency-domain block interleaving (FDI) in combination with forward error correction (FEC) coding to combat periodic impulsive noise [6]. The FDI-OFDM transmitter contains a sample-level interleaver across multiple OFDM symbols in the frequency domain, i.e., before the inverse discrete Fourier transform (IDFT). The corresponding deinterleaver at the receiver effectively spreads the bursty errors into isolated errors over a large number of OFDM symbols, in order to reduce their impact on bit error rate (BER) in coded systems. Alternate designs adopt time-domain block interleaving (TDI) [9], where the signal is interleaved and deinterleaved in the time domain, i.e., post-IDFT at the transmitter and pre-DFT at the receiver. The deinterleaver at the receivers scatters noise bursts into short isolated impulses in the time domain (Fig. 2). TDI-OFDM achieves superior BER improvement over FDI-OFDM in high SNR regimes (e.g. above 10 or 20dB, depending on specific noise scenarios), whereas FDI-OFDM performs better towards lower SNRs [9].

To further compensate the communication performance loss due to non-AWGN statistics of the noise, receiver methods that exploit statistical properties of periodic impulsive noise have been investigated. In [10], cyclic spectrum analysis was used to detect and extract second-order cyclostationary

process. A linear MMSE frequency domain equalizer was derived for single-carrier OFDM systems in cyclostationary noise [11]. Recent studies targeting NB PLC proposed adaptive error prediction filters [12], [13] and noise whitening filters [14] to mitigate periodic impulsive noise in the time domain. These parametric methods assume a specific statistical model of the noise, and estimate model parameters by training. Unfortunately, parameter estimation for periodic impulsive noise is generally of high complexity. This is because of the significant increase in the number of parameters, and hence the degrees of freedom, in order to capture the non-negligible time-domain correlation in periodic impulsive noise. Accurate estimation of these parameters generally requires a large amount of data, i.e., over multiple cycles, which entails not only significant training overhead, but also a large memory typically not present in current PLC modems. Furthermore, the increased degrees of freedom makes the estimation more vulnerable to outliers.

Non-parametric methods, on the other hand, do not make any assumptions on statistical models of the noise and hence do not require any training overhead. Our previous work [8], [15] on mitigating asynchronous impulsive noise, which consists of short impulses with random occurrence, developed two non-parametric algorithms to estimate and subtract the noise impulses from received OFDM signal. The idea was to exploit the sparse structure of the noise in the time domain and formulate a compressed sensing problem, where the sparse noise vector can be estimated by observing various subcarriers (a.k.a. tones) of a received OFDM symbol. We then solved the compressed sensing problem using sparse Bayesian learning (SBL) techniques [16].

In this paper, we aim to develop non-parametric receiver methods to mitigate periodic impulsive noise in TDI-OFDM systems for NB PLC. Towards this end, we first describe our system model in Section II. After introducing the SBL algorithm in Section III, we briefly review our previously developed SBL-based methods in Section IV-A and show that these methods can be applied to mitigate periodic impulsive noise in TDI-OFDM systems. Then in Section IV-B we extend the SBL-based methods to a novel closed loop algorithm that exploits decision feedback from the decoder to further improve the communication performance.

II. SYSTEM MODEL

We consider a TDI-OFDM system [9] whose complex baseband equivalent representation is shown in Fig. 3. At the transmitter, binary data packets are encoded and mapped to OFDM symbols, each with M non-data tones and $N - M$ data tones. The non-data tones are either null tones for spectral shaping and inter-carrier interference reduction, or pilots for channel estimation and synchronization. An OFDM symbol, denoted by \mathbf{x} , is converted to the time domain by IDFT. After the IDFT, multiple OFDM symbols are interleaved using a sample-level block interleaver. A cyclic prefix (CP), assumed to be longer than the channel delay spread, is inserted to the beginning of each OFDM symbol to prevent inter-symbol interference. Inserting the CP after the interleaver maintains the cyclic structure within each transmitted OFDM symbol, and hence the received signal after CP removal is the circular convolution of the transmitted signal with the multipath channel. Similarly to conventional OFDM systems, such

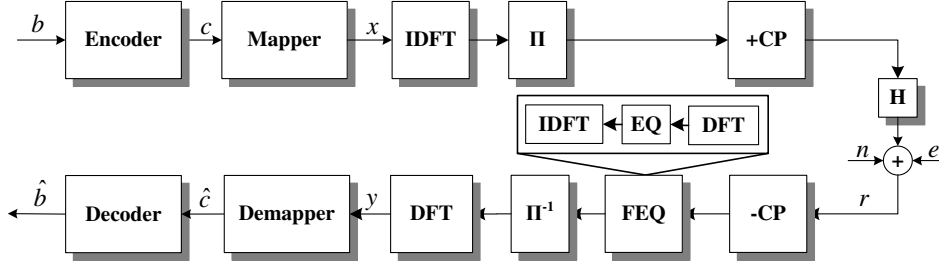


Fig. 3. A time-domain interleaved OFDM system. Π denotes the sample-level interleaver, and Π^{-1} the corresponding deinterleaver.

signal can be equalized by one-tap frequency-domain channel equalizers (FEQ). The equalized signal is then deinterleaved before converted to the frequency domain by DFT. Assuming perfect channel estimation, the demodulated OFDM signal \mathbf{y} can be expressed as

$$\mathbf{y} = \mathbf{x} + \mathbf{F}\mathbf{e}_\pi + \mathbf{F}\mathbf{n}_\pi = \mathbf{x} + \mathbf{F}\mathbf{e}_\pi + \mathbf{g}_\pi. \quad (1)$$

Here \mathbf{F} is the N -point DFT matrix, \mathbf{e}_π and \mathbf{n}_π denote the time-domain impulsive noise and additive Gaussian noise after deinterleaving, and we have defined $\mathbf{g}_\pi \triangleq \mathbf{F}\mathbf{n}_\pi$. Note that although the AWGN \mathbf{n} in Fig. 3 is spectrally shaped by the FEQ, it becomes less correlated in the time domain after the block deinterleaver and hence \mathbf{n}_π , as well as \mathbf{g}_π , can be well approximated by AWGN.

Let \mathcal{I} denote the index set of the null and pilot tones, where $|\mathcal{I}| = M < N$. Also, let $(\cdot)_{\mathcal{I}}$ denote the sub-matrix (or sub-vector) corresponding to the rows (or elements) indexed by the set \mathcal{I} . The impulsive noise can be observed from the null and pilot tones of the received OFDM symbol, since

$$\begin{aligned} \mathbf{z} &\triangleq \mathbf{y}_{\mathcal{I}} - \mathbf{x}_{\mathcal{I}} \\ &= \mathbf{F}_{\mathcal{I}}\mathbf{e}_\pi + \mathbf{g}_{\mathcal{I}}, \\ \mathbf{g}_{\mathcal{I}} &\sim \mathcal{CN}(\mathbf{0}, \sigma^2\mathbf{I}_M), \end{aligned} \quad (2)$$

where $\mathbf{x}_{\mathcal{I}}$ contains elements that are either zero or known pilots. Note that we have dropped the subscript π in \mathbf{g}_π for conciseness purposes.

The recovery of the length- N vector \mathbf{e}_π from the noisy underdetermined $M \times N$ linear system is generally an ill-conditioned problem. However, if the time-domain deinterleaved noise \mathbf{e}_π has a sparse structure, it could be accurately estimated by compressed sensing techniques from (2). Let us define the sparsity of a vector as the percentage of non-zero elements. In compressed sensing algorithms, lower sparsity of \mathbf{e}_π generally leads to improved recovery performance.

Given a particular noise scenario, the size of the interleaver is an important design factor that determines the sparseness of \mathbf{e}_π and therefore the performance of the SBL-based algorithms. The key is to maintain the sparseness of \mathbf{e}_π (i.e., number of non-zero elements) below a certain level that allows accurate estimation by the SBL techniques. In NB PLC systems, the interleaving can be done over an entire packet, which contains up to 56 QPSK modulated OFDM symbols according to the G3 standard in the CENELEC-A band. This gives a maximum interleaver size of 38.92 *ms*, spanning about 2.3 AC cycles in the US, or equivalently 4.6 noise periods. The maximum packet duration will be doubled in BPSK modulation and even

larger when repetition code is used. As such, we claim that the assumption of having a large interleaver with the size approximately equal to integer multiples of the noise period is realistic in NB PLC systems. Such interleavers will result in \mathbf{e}_π with sparseness typically ranging from 10% to 30%, which can be accurately recovered by the SBL-based algorithms, as will be demonstrated by the simulation results.

We would like to use the estimated impulsive noise to improve the detection of \mathbf{x} . More specifically, the impulsive noise estimate $\hat{\mathbf{e}}_\pi$ can be subtracted from the received symbol on the data tones to form a new decision metric

$$\begin{aligned} \hat{\mathbf{y}}_{\bar{\mathcal{I}}} &= \mathbf{y}_{\bar{\mathcal{I}}} - \mathbf{F}_{\bar{\mathcal{I}}}\hat{\mathbf{e}}_\pi \\ &= \mathbf{x}_{\bar{\mathcal{I}}} + \mathbf{g}_{\bar{\mathcal{I}}} + \mathbf{F}_{\bar{\mathcal{I}}}(\mathbf{e}_\pi - \hat{\mathbf{e}}_\pi). \end{aligned} \quad (3)$$

where $\bar{(\cdot)}$ indicates set complement and thus $\bar{\mathcal{I}}$ indicates the set of data tone indices. Assuming that $\hat{\mathbf{e}}_\pi \approx \mathbf{e}_\pi$, the receiver can then proceed as if only AWGN were present and apply the conventional detection and decoding algorithms.

III. SPARSE BAYESIAN LEARNING

Among various compressed sensing algorithms, sparse Bayesian learning (SBL) has become increasingly attractive due to its improved robustness over deterministic approaches such as Basis Pursuit [17]. SBL was first proposed by Tipping [18], and was introduced to sparse signal recovery by Wipf and Rao in [16].

Generally, SBL is a Bayesian learning approach for solving the linear regression problem

$$\mathbf{t} = \Phi\mathbf{w} + \mathbf{v}, \quad \mathbf{v} \sim \mathcal{CN}(\mathbf{0}, \sigma^2\mathbf{I}_M), \quad (4)$$

where \mathbf{t} is an observation vector, $\Phi \in \mathcal{C}^{M \times N}$ is an overcomplete basis (i.e., $M < N$), and \mathbf{w} is a sparse weight vector to be estimated.

SBL imposes a parameterized Gaussian prior on \mathbf{w}

$$p(\mathbf{w}; \Gamma) = \mathcal{CN}(\mathbf{w}; \mathbf{0}, \Gamma), \quad (5)$$

where $\Gamma \triangleq \text{diag}\{\gamma\}$, and $\gamma \in \mathcal{R}^N$ whose i -th component γ_i is the variance of w_i . Given the prior, the likelihood of the observation can be expressed as

$$p(\mathbf{t}; \Gamma, \sigma^2) = \mathcal{CN}(\mathbf{t}; \mathbf{0}, \Phi\Gamma\Phi^* + \sigma^2\mathbf{I}_M). \quad (6)$$

A maximum likelihood (ML) estimator solves the hyperparameters γ and σ^2 that maximize (6). The ML solution is computed iteratively using expectation maximization (EM), treating \mathbf{w} as the latent variable.

Given the observations and the estimated hyperparameters, the posterior density of \mathbf{e} is also a Gaussian distribution

$$\begin{aligned} p(\mathbf{w}|\mathbf{t}; \Gamma, \sigma^2) &= \mathcal{CN}(\mathbf{w}; \boldsymbol{\mu}_w, \boldsymbol{\Sigma}_w), \\ \boldsymbol{\mu}_w &= \sigma^{-2} \boldsymbol{\Sigma}_w \boldsymbol{\Phi}^* \mathbf{t}, \\ \boldsymbol{\Sigma}_w &= (\sigma^{-2} \boldsymbol{\Phi}^* \boldsymbol{\Phi} + \Gamma^{-1})^{-1}. \end{aligned} \quad (7)$$

The maximum *a posteriori* (MAP) estimate of \mathbf{w} is the posterior mean $\boldsymbol{\mu}_w$.

Due to the sparsity promoting property of the prior, upon convergence, most components of $\boldsymbol{\gamma}$ and hence $\boldsymbol{\mu}_w$ are driven to zero, rendering a sparse estimate of \mathbf{w} . It has been shown in [16] that SBL has improved robustness compared to other deterministic compressed sensing algorithms such as Basis Pursuit [17] and FOCUSS [19].

IV. NON-PARAMETRIC NOISE MITIGATION METHODS

In this section, we first briefly review the two SBL-based impulsive noise mitigation methods we previously developed [15]. Although initially designed for mitigating asynchronous impulsive noise, these methods can also be applied to mitigate periodic impulsive noise in TDI-OFDM systems, since the compressed sensing problem in (2) takes exactly the same form as that in [15]. Then we extend the methods to a novel closed-loop algorithm that exploits decision feedback from the decoder to further improve the robustness of the noise estimator in the presence of long noise bursts.

A. Open Loop Noise Estimation Methods

The SBL technique can be directly applied to estimate the deinterleaved periodic impulsive noise \mathbf{e}_π from the null and pilot tones of the received OFDM symbol. Substituting $\mathbf{t} = \mathbf{z}$, $\boldsymbol{\Phi} = \mathbf{F}_\mathcal{I}$, $\mathbf{w} = \mathbf{e}_\pi$, and $\mathbf{v} = \mathbf{g}_\mathcal{I}$ into (4) gives exactly (2). We therefore apply SBL to obtain the MAP estimate of $\hat{\mathbf{e}}_\pi$ and subtract it from the received signal according to (3).

The robustness of the noise estimator using null and pilot tones is affected by the number of null and pilot tones in an OFDM symbol, and the sparsity of \mathbf{e}_π . With a fixed number of null and pilot tones, as the number of non-zero elements in \mathbf{e}_π increases to above a certain threshold, the problem becomes ill-conditioned and hence significant estimation error could be incurred. In periodic impulsive noise with long bursts, after appropriate deinterleaving, \mathbf{e}_π might not be sparse enough to guarantee successful recovery from the observation on null and pilot tones. To improve the robustness of the noise estimator in the presence of long noise bursts, it is desirable to exploit more information from received signal.

A simple way to do this is to exploit information available on data tones. We define $\mathbf{u} \triangleq \mathbf{x} + \mathbf{g}$, and augment the observation vector \mathbf{z} by the data tones of received signal, i.e.,

$$\begin{aligned} \begin{bmatrix} \mathbf{z} \\ \mathbf{y}_{\bar{\mathcal{I}}} \end{bmatrix} &= \mathbf{F} \mathbf{e}_\pi + \begin{bmatrix} \mathbf{u}_\mathcal{I} \\ \mathbf{u}_{\bar{\mathcal{I}}} \end{bmatrix}, \\ \mathbf{u}_\mathcal{I} &\sim \mathcal{CN}(\mathbf{0}, \sigma^2 \mathbf{I}_M), \\ \mathbf{u}_{\bar{\mathcal{I}}} &\sim \mathcal{CN}(\mathbf{x}_{\bar{\mathcal{I}}}, \sigma^2 \mathbf{I}_{N-M}). \end{aligned} \quad (8)$$

The system model in (8) has the same form as (1), with an additional hyperparameter $\mathbf{x}_{\bar{\mathcal{I}}}$. Although $\mathbf{x}_{\bar{\mathcal{I}}}$ consists of constellation points (i.e., they are discrete values), to estimate it

by the EM algorithm, we temporarily relax it to be continuous. Upon convergence of the EM algorithm, we make a hard decision on $\mathbf{x}_{\bar{\mathcal{I}}}$ before passing it to the convolutional decoder.

B. A Closed Loop Noise Estimation Method

The open loop noise estimation methods exploit information in various tones of the received OFDM symbol. In coded systems, the decision feedback from the convolutional decoder could also be utilized as side information to aid the noise estimation. The SBL framework makes it convenient to integrate such side information. To do this, we impose a prior distribution on the hyperparameters Γ , or equivalently on the precision matrix $\mathcal{T} \triangleq \Gamma^{-1}$. Let $\boldsymbol{\tau} \triangleq [\tau_1, \dots, \tau_N]^T$ denote the vector formed by the diagonal elements of \mathcal{T} . The conjugate prior on $\boldsymbol{\tau}$ is a Gamma distribution

$$P(\boldsymbol{\tau}; \mathbf{a}, \mathbf{b}) = \prod_{i=1}^N \text{Ga}(\tau_i; a_i, b_i). \quad (9)$$

where $\text{Ga}(\cdot; a, b)$ denotes the pdf of the Gamma distribution with parameters a and b . When $a_i = 0, b_i = 0, \forall i$, (9) reduces to a uniform distribution, which is a non-informative prior implicitly imposed in the previously described SBL framework. Non-zero values of a_i and b_i contain prior information that can be integrated into the likelihood function of \mathbf{z} , resulting in

$$p(\mathbf{z}; \mathcal{T}, \sigma^2, \mathbf{a}, \mathbf{b}) = \mathcal{CN}(\mathbf{z}; \mathbf{0}, \mathbf{F}_\mathcal{I} \mathcal{T}^{-1} \mathbf{F}_\mathcal{I}^* + \sigma^2 \mathbf{I}_M) \times \text{Ga}(\boldsymbol{\tau}; \mathbf{a}, \mathbf{b}). \quad (10)$$

The maximum likelihood (ML) estimate of τ_i can be solved individually as

$$\tau_i = \gamma_i^{-1} = \frac{1 + 2a_i}{\boldsymbol{\mu}_{\mathbf{e},i}^2 + \boldsymbol{\Sigma}_{\mathbf{e},ii} + 2b_i}, \quad (11)$$

where $\boldsymbol{\mu}_{\mathbf{e}}$ and $\boldsymbol{\Sigma}_{\mathbf{e}}$ denote the posterior mean and covariance of \mathbf{e}_π given \mathbf{z} and the values of hyperparameters in the current iteration. We can see the prior information contained in a_i and b_i does affect the ML estimates of $\boldsymbol{\gamma}$. Since (11) is the conjugate prior on $\boldsymbol{\tau}$, the posterior probability of $\boldsymbol{\tau}$ given $\mathbf{e}_\pi, \mathbf{a}$ and \mathbf{b} is also Gamma distributed, i.e.,

$$P(\boldsymbol{\tau} | \mathbf{e}_\pi; \mathbf{a}, \mathbf{b}) = \prod_{i=1}^N \text{Ga}(\tau_i; \tilde{a}_i, \tilde{b}_i) \quad (12)$$

with the updated parameters

$$\begin{aligned} \tilde{a}_i &= a_i + \frac{1}{2}, \\ \tilde{b}_i &= b_i + \frac{|e_{\pi,i}|^2}{2}. \end{aligned} \quad (13)$$

Suppose that in addition to the MAP estimate $\hat{\mathbf{e}}_\pi$ given by the estimator using null and pilot tones, a second estimate of \mathbf{e}_π , denoted by $\hat{\mathbf{e}}'_\pi$, is available based on certain side information. The side information contained in $\hat{\mathbf{e}}'_\pi$ can be fused into $\hat{\mathbf{e}}_\pi$ via the posterior distribution of $\boldsymbol{\tau}$ given $\hat{\mathbf{e}}'_\pi$. More specifically, given $\hat{\mathbf{e}}'_\pi$, we update \mathbf{a} and \mathbf{b} according to (13), and then solve the ML estimate of $\boldsymbol{\tau}$ (11) with the updated values of $\tilde{\mathbf{a}}$ and $\tilde{\mathbf{b}}$.

In coded OFDM systems, the redundancy in the coded signal on the data tones can be exploited as the side information to

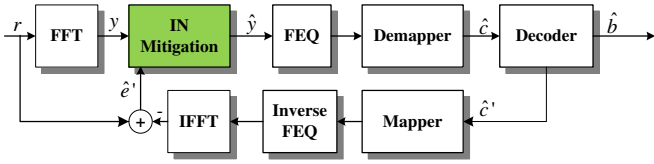


Fig. 4. A closed loop periodic impulsive noise estimator using decision feedback from the decoder.

provide a second estimate of \hat{e}'_{π} . More specifically, the decoder takes the OFDM symbols after impulsive noise mitigation as the input, and produces hard decisions on the uncoded and coded bits, $\hat{\mathbf{b}}$ and $\hat{\mathbf{c}}$, respectively. Using $\hat{\mathbf{c}}$ we can recover the data tones of the OFDM symbols by appropriate constellation mapping. This gives an estimate of $\hat{\mathbf{x}}_{\overline{T}}$, which is transformed to the time domain and subtracted from the received signal \mathbf{r} to generate the estimate of \hat{e}'_{π} . Then we use \hat{e}'_{π} to update \mathbf{a} and \mathbf{b} , through which the information extracted from the coding redundancy is transferred back to the impulsive noise estimator. As such, we form a decision feedback estimator that transfers information back-and-forth between the impulsive noise estimator using null and pilot tones and the decoder using data tones (Fig. 4). Compared to the estimator using all tones, the decision feedback estimator is expected to have better performance by exploiting the redundant information (i.e., coding structure) on the data tones.

V. SIMULATION RESULTS

To evaluate the performance of our non-parametric noise estimation methods, we simulate a complex baseband TDI-OFDM system over a flat channel. The system parameters are listed in Table I and compared with those in the G3 standard operating in the CENELEC-A band.

We generate periodic impulsive noise using the LPTV system model in [4]. We divide one period of the noise into three intervals, each assuming an individual spectral shape (Fig. 1). The spectral shapes are fitted to noise measurement collected at an outdoor low-voltage site as shown in [4]. We vary the duration of noise bursts (i.e., the total duration of the second and the third intervals) from 10% to 30% of a period.

In periodic impulsive noise, we simulate our proposed algorithms in a coded TDI-OFDM system, and compare their BER performance with both TDI-OFDM and FDI-OFDM systems without noise mitigation. In both TDI and FDI OFDM systems, we use two interleaver sizes, one spanning approximately half an AC cycle (i.e., one period of the noise), and the other about

Parameters	Simulation	G3 in CENELEC-A
Sampling Frequency	400 kHz	400 kHz
FFT Length	128	256
Modulation	QPSK	DQPSK
# of Tones	128	128
# of Data Tones	72	36
# of Null Tones	56	92
FEC code	Rate-1/2 Convolutional	Rate-1/2 Convolutional
Interleaver	TDI or FDI	FDI
Interleave Size	0.5-1 AC cycles	up to about 2 AC cycles

TABLE I. PARAMETERS OF THE SIMULATED COMPLEX BASEBAND OFDM SYSTEM AND THE REAL PASSBAND OFDM SYSTEM USING DQPSK MODULATION IN THE G3 STANDARD OPERATING IN THE CENELEC-A BAND.

an entire AC cycle. Both interleaver sizes are smaller than the maximum interleaver size in G3, which according to Section II spans 2.3 AC cycles.

With the interleaver size fixed at approximately an AC cycle, we increase the noise burst duration from 10% to 30% of a period. The BER performance of all algorithms are plotted in Fig. 5. Without any noise mitigation, the TDI-OFDM system performs worse than the conventional FDI-OFDM system until the SNR reaches 9 dB in the 10% burst case. This corresponds well to the results in [9] that the BER improvement of TDI-OFDM over FDI-OFDM can only be achieved above certain SNR threshold. By embedding the three SBL-based denoising algorithms into the TDI-OFDM framework, we are able to lower such SNR threshold to 6 dB, 0 dB and -3 dB, respectively. As the length of noise bursts increases to 30% of a period, the TDI-OFDM system without noise mitigation starts to show BER improvement over the FDI-OFDM system earlier at 7 dB. Embedding our SBL-based estimators into the TDI-OFDM system, especially the ones using all tones and decision feedback, further lowers the SNR threshold to about -1.5 dB and -4 dB, respectively. We notice that the SNR gains obtained by our proposed algorithms over the TDI-OFDM system itself are smaller than in the previous 10% burst case. The SBL algorithm using null tones even performs slightly worse than the TDI-OFDM system without noise mitigation as the SNR grows above 6.5 dB. The reason is that in the 30% burst case, after deinterleaving, the number of impulses per OFDM symbol increases to a level where the performance of the SBL technique begins to saturate.

To demonstrate the robustness of our proposed algorithms to different interleaver sizes, we simulate the algorithms with a shorter interleaver spanning about half an AC cycle, while fixing the noise burst duration to 30% of a period. Since both interleaver sizes are an integer multiple of the noise period, in theory, after the deinterleaving, the noise within an OFDM symbol should have the same average sparseness. Therefore the same BER performance can be expected from our proposed

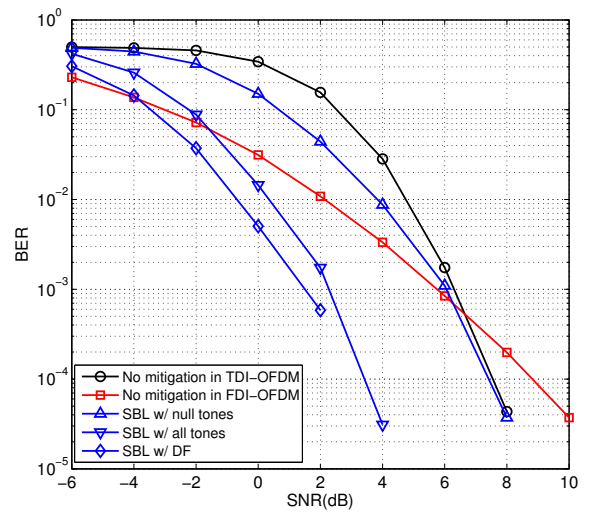


Fig. 6. Coded bit error rate (BER) performance of the proposed algorithms in periodic impulsive noise, in comparison with the TDI-OFDM and FDI-OFDM systems without noise mitigation. The interleaving is done over half an AC cycle. The burst interval is fixed at 30% of a period.

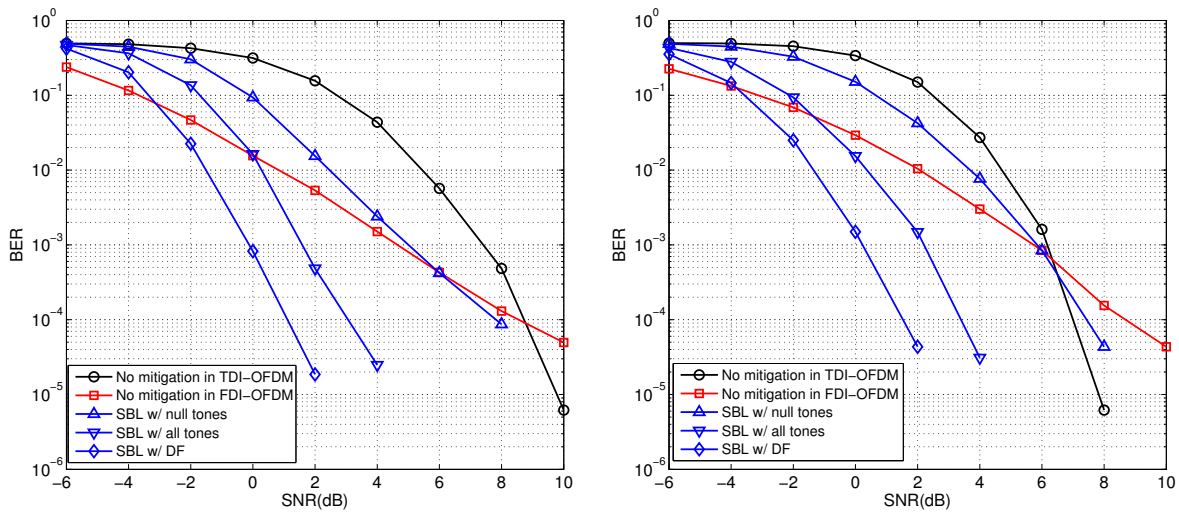


Fig. 5. Coded BER performance of the proposed algorithms in periodic impulsive noise, in comparison with the TDI-OFDM and FDI-OFDM systems without noise mitigation. The interleaving is done over an entire AC cycle. The burst interval varies from 10% (left) to 30% (right) of a period.

algorithms. Comparing the BER performance in Fig. 6 to Fig. 5, we observe that decreasing the interleaver size leads to negligible effects on all BER curves, except for the marginal BER loss for the TDI-OFDM system without noise mitigation at SNRs above 6dB. This is because the TDI-OFDM system itself assumes AWGN, and a larger interleaver is useful to make noise samples within an OFDM symbol less correlated, i.e., closer to AWGN in statistics.

VI. CONCLUSION

This paper presents three non-parametric methods for improving communication performance of time-domain interleaved OFDM systems for NB PLC in the presence of periodic impulsive noise. We exploit the sparse structure of the deinterleaved impulsive noise in the time domain, and apply sparse Bayesian learning (SBL) techniques to estimate the impulsive noise from the received signal by observing information on various subcarriers and by utilizing decision feedback from the decoder. All the methods are non-parametric; i.e., they do not require prior knowledge on the statistical noise model or model parameters. We validate the proposed algorithms based on simulated periodic impulsive noise.

REFERENCES

- [1] S. Galli, A. Scaglione, and Z. Wang, "For the grid and through the grid: The role of power line communications in the smart grid," *Proc. of the IEEE*, vol. 99, no. 6, pp. 998–1027, 2011.
- [2] A. Moscatelli, "Technologies evolution for smart grid applications," in *IEEE Int. Symp. Power Line Comm. and Appl.*, 2011. [Online]. Available: <http://www.ieee-isplc.org/2011/programme.html#keynotes>
- [3] M. Katayama, T. Yamazato, and H. Okada, "A mathematical model of noise in narrowband power line communication systems," *IEEE J. Sel. Areas Comm.*, vol. 24, no. 7, pp. 1267–1276, 2006.
- [4] M. Nassar, A. Dabak, I. H. Kim, T. Pande, and B. L. Evans, "Cyclostationary noise modeling in narrowband powerline communication for smart grid applications," *Proc. IEEE Int. Conf. on Acoustics, Speech and Sig. Proc.*, pp. 3089–3092, 2012.
- [5] K. F. Nieman, J. Lin, M. Nassar, K. Waheed, and B. L. Evans, "Cyclic spectral analysis of power line noise in the 3-200 kHz band," in *Proc. IEEE Int. Symp. Power Line Comm. and Appl.*, 2013.
- [6] M. Nassar, J. Lin, Y. Mortazavi, A. Dabak, I. H. Kim, and B. L. Evans, "Local utility power line communications in the 3-500 khz band: Channel impairments, noise, and standards," *IEEE Sig. Proc. Mag.*, vol. 29, no. 5, pp. 116–127, 2012.
- [7] Texas Instruments, "Data sheet for powerline communications analog front-end AFE031," 2012. [Online]. Available: <http://www.ti.com/lit/ds/symlink/afe031.pdf>
- [8] J. Lin, M. Nassar, and B. L. Evans, "Impulsive noise mitigation in powerline communications using sparse Bayesian learning," *IEEE J. Sel. Areas Comm.*, vol. 31, no. 7, pp. 1172–1183, 2013.
- [9] A. Al-Dweik, A. Hazmi, B. Sharif, and C. Tsimenidis, "Efficient interleaving technique for OFDM system over impulsive noise channels," in *Proc. IEEE Int. Symp. Pers. Indoor and Mobile Radio Comm.*, 2010.
- [10] W. Gardner and C. Spooner, "The cumulant theory of cyclostationary time-series. I. Foundation," *IEEE Trans. Sig. Proc.*, vol. 42, no. 12, pp. 3387–3408, 1994.
- [11] Y. Yoo and J. Cho, "Asymptotic analysis of CP-SC-FDE and UW-SC-FDE in additive cyclostationary noise," *Proc. IEEE Int. Conf. Comm.*, pp. 1410–1414, 2008.
- [12] R. Garcia, L. Díez, J. Cortes, and F. Canete, "Mitigation of cyclic short-time noise in indoor power-line channels," *Proc. IEEE Int. Symp. Power Line Comm. and Appl.*, pp. 396–400, 2007.
- [13] A. Liano, A. Sendin, A. Arzuaga, and S. Santos, "Quasi-synchronous noise interference cancellation techniques applied in low voltage PLC," *Proc. IEEE Int. Symp. Power Line Comm. and Appl.*, 2011.
- [14] J. Lin and B. L. Evans, "Cyclostationary noise mitigation in narrowband powerline communications," *Proc. APSIPA Annual Summit Conf.*, 2012.
- [15] J. Lin, M. Nassar, and B. L. Evans, "Non-parametric impulsive noise mitigation in OFDM systems using sparse Bayesian learning," *Proc. IEEE Global Comm. Conf.*, 2011.
- [16] D. Wipf and B. Rao, "Sparse Bayesian learning for basis selection," *IEEE Trans. Signal Process.*, vol. 52, no. 8, pp. 2153–2164, 2004.
- [17] S. Chen, D. Donoho, and M. Saunders, "Atomic decomposition by basis pursuit," *SIAM review*, vol. 43, no. 1, pp. 129–159, 2001.
- [18] M. Tipping, "Sparse Bayesian learning and the relevance vector machine," *J. Mach. Learn. Res.*, vol. 1, pp. 211–244, 2001.
- [19] I. Gorodnitsky and B. Rao, "Sparse signal reconstruction from limited data using FOCUSS: A re-weighted minimum norm algorithm," *IEEE Trans. Sig. Proc.*, vol. 45, no. 3, pp. 600–616, 2002.